

Article

Behavior-Aware Aggregation of Distributed Energy Resources for Risk-Aware Operational Scheduling of Distribution Systems

Mingyue He ¹, Zahra Soltani ¹, Mojdeh Khorsand ^{1,*}, Aaron Dock ², Patrick Malaty ² and Masoud Esmaili ¹

¹ Department of Electrical, Computer and Energy Engineering, Arizona State University, Tempe, AZ 85287, USA

² Salt River Project (SRP) Power and Water, 1500 N. Mill Ave., Tempe, AZ 85288, USA

* Correspondence: mojdeh.khorsand@asu.edu

Abstract: Recently there has been a considerable increase in the penetration level of distributed energy resources (DERs) due to various factors, such as the increasing affordability of these resources, the global movement towards sustainable energy, and the energy democracy movement. However, the uncertainty and variability of DERs introduce new challenges for power system operations. Advanced techniques that account for the characteristics of DERs, i.e., their intermittency and human-in-the-loop factors, are essential to improving distribution system operations. This paper proposes a behavior-aware approach to analyze and aggregate prosumers' participation in demand response (DR) programs. A convexified AC optimal power flow (ACOPF) via a second-order cone programming (SOCP) technique is used for system scheduling with DERs. A chance-constrained framework for the system operation is constructed as an iterative two-stage algorithm that can integrate loads, DERs' uncertainty, and SOCP-based ACOPF into one framework to manage the violation probability of the distribution system's security limits. The benefits of the analyzed prosumers' behaviors are shown in this paper by comparing the optimal system scheduling with socially aware and non-socially aware approaches. The case study illustrates that the socially aware approach within the chance-constrained framework can utilize up to 43% more PV generation and improve the reliability and operation of distribution systems.

Keywords: AC optimal power flow; chance constraints; distributed energy resources; human-in-the-loop; risk aware; socially aware; sociodemographic information



Citation: He, M.; Soltani, Z.; Khorsand, M.; Dock, A.; Malaty, P.; Esmaili, M. Behavior-Aware Aggregation of Distributed Energy Resources for Risk-Aware Operational Scheduling of Distribution Systems. *Energies* **2022**, *15*, 9420. <https://doi.org/10.3390/en15249420>

Academic Editors: Vincent Reinbold, Simon Meunier and Adrien Voltaire

Received: 20 October 2022

Accepted: 8 December 2022

Published: 13 December 2022

Publisher's Note: MDPI stays neutral with regard to jurisdictional claims in published maps and institutional affiliations.



Copyright: © 2022 by the authors. Licensee MDPI, Basel, Switzerland. This article is an open access article distributed under the terms and conditions of the Creative Commons Attribution (CC BY) license (<https://creativecommons.org/licenses/by/4.0/>).

1. Introduction

1.1. Motivation and Background

The proliferation of distributed energy resources (DERs) in smart grids has changed the traditionally passive role of electricity consumers to that of active participants, i.e., prosumers (both consumers and producers). Demand response (DR), as a type of DER, can assist with overcoming some of the recent challenges of smart grids, e.g., offsetting the uncertainty of variable energy resources (VERs). Even though residential customers have great DR potential, their large numbers and the complexity of predicting their consumption behaviors make it challenging to model and leverage their DR potential. The system scheduling considering DR programs is usually conducted for aggregated groups of prosumers [1–4]. However, randomly aggregating DR resources without considering their critical features cannot fully leverage their DR potential. One of these important features is the human-in-the-loop (HITL) characteristic of residential DR, which is also one of the key contributors to the challenges of DR prediction and management. Research in the social science realm has shown that the electricity consumption behavior of prosumers is closely tied to their demographic characteristics, e.g., income level, number of occupants in their household, and number of children [1]. The consideration of HITL factors can significantly

enhance the assessment of prosumers' participation in DR programs. Some prior works have considered HITL factors by establishing different functions or training machine learning models, such as in [5–7]. However, a few functions may not be general enough for all prosumers, and machine learning models are black boxes to system operators, which may not be preferred by system operators. To fill these gaps, a combination of machine learning models using prosumers' historical data and an advanced aggregation method while accounting for the selected demographic characteristics is proposed.

Since the ratio of R/X in distribution systems is higher than that in transmission systems, assumptions of DC optimal power flow are not valid for distribution system scheduling. AC optimal power flow (ACOPF) models are essential for scheduling distribution systems with DERs. However, non-linear and non-convex ACOPF models are not preferred because the solution obtained from these models may not be the global optimal solution and can be easily intractable. Relaxed convex models, such as second-order cone programming (SOCP) or semidefinite programming (SDP), can provide the global optimal solution within a tractable computation time. The exactness of SOCP and SDP relaxation has been studied in [8–11], and sufficient conditions of exactness have been proposed and proved. References [8–11] show that SDP and SOCP are equivalent for solving OPF problems in radial distribution networks. Moreover, SOCP is more computationally efficient compared to SDP [8–11]. Therefore, the SOCP-based ACOPF model is used in this paper and embedded in a chance-constrained framework for distribution system scheduling.

Although DERs, including DR and rooftop photovoltaic (PV) units, offer promising solutions, e.g., for resiliency and environmental concerns, their integration into power systems imposes operational challenges due to their intermittent energy production. The traditional solutions to overcome the intermittency of DERs mainly rely on a higher amount of reserve procurement from bulk (and potentially polluting and expensive) generators. Such solutions can negate some of the benefits of the high penetration level of DERs. Moreover, voltage management in distribution networks with a high penetration level of intermittent DERs is critical. Risk-aware operational methods, e.g., chance-constrained and robust optimization models, are essential to enhance the distribution system operation considering the intermittency of DERs. However, those models that account for uncertainty are generally complex and computationally expensive. For example, robust optimization and chance-constrained models can account for uncertainty; however, robust optimization is only computationally tractable with a well-prepared uncertainty set, and the computational time of a traditional chance-constrained model can exponentially increase as the number of scenarios increases, which makes it intractable with many scenarios in a large network. Thus, a model that is easy to solve and able to incorporate different DERs' uncertainties and evaluation methods (e.g., the socially aware method in this paper) is proposed to account for the integration and uncertainty of DERs and improve the distribution system's operation.

To address these challenges, this paper proposes a method and solution for the following research questions:

- How can prosumers' consumption behavior be modeled using historical observations and via a behavior-aware approach?
- How can an advanced aggregation approach improve the estimation of DR participation?
- How can behavior-aware DR analyses and enhanced DR aggregation strategies improve power system operations?
- How can risk-aware operational strategies be utilized to account for the uncertainty of diverse groups of DR prosumers, loads, and other DERs into one framework?

1.2. Literature Review and Contributions

Prior work has proposed different approaches to predict and model the energy consumption behavior of customers based on demographic characteristics. A survey-less model is proposed in [1] using Mosaic data to classify households into segments based on their demographic factors, such as income level and family composition, and geode-

mographic information. Reference [2] uses a decision tree to classify customers based on their sociodemographic data to predict their consumption. Reference [3] shows that the prediction of residential customers' energy usage can be improved by utilizing their socioeconomic and demographic characteristics. The authors in [4] propose hierarchical clustering methodologies to classify customers based on dissimilarity measures and customers' consumption. In addition, they show that the clustering results match with demographic segments in [4]. The sociodemographic information of customers is used in [12] to predict the baseline consumption (before DR) to analyze their on-peak DR participation. The efficacy of using sociodemographic information in a DR analysis is also shown in [12]. Reference [13] shows that customers' demographic data can be used to enhance the estimation of the charging behavior of plug-in electric vehicles (EVs), which results in reducing stress on the distribution system. The authors in [14] investigate residential customers' temporal consumption patterns using their demographic and appliance stock characteristics in a hidden Markov model. The references [1–4] and [12–14] show that demographic characteristics are key factors that contribute to customers' consumption behavior. However, these studies do not pursue behavior-aware or socially aware aggregation strategies and do not analyze the impact of such enhanced aggregation approaches on system operations and energy and reserve scheduling for distribution grids; this important enhancement is critical as it follows the recommendation of FERC order 2222 that states small DER resources should be properly aggregated for practical participation in a system's operation [15].

Convex ACOPF models are employed for distribution systems in the literature. References [16,17] utilize the SOCP technique to achieve a convex relaxation of ACOPF based on the bus injection and branch flow models. Reference [9] proposes a deterministic multi-period SOCP-based ACOPF for EV planning and provides a sufficient condition for the exactness of SOCP-based ACOPF. In [18], an ACOPF model with DERs and voltage regulation transformers is convexified by a chordal relaxation-based SDP model. The restoration of a distribution system via multiple microgrids is formulated in [19] as a mixed-integer SOCP problem by relaxing the rank constraint of the coefficient matrix. References [9,16–19] propose well-established convex ACOPF for distribution grid operation; however, these studies could be enhanced by considering DER integration and uncertainty modeling.

One of the common approaches for the uncertainty modeling of intermittent resources is robust optimization. References [20,21] utilize robust optimization for the multi-period ACOPF model to account for the uncertainty of loads and DERs. However, robust optimization is generally computationally expensive [20,21]. For example, the robust model in [21] with three different uncertainty sets takes 2.5, 6.4, and 16.2 h to solve for a small system, i.e., a 37-bus system. Some prior works apply chance-constrained models for the uncertainty modeling of DERs in the ACOPF problem. For instance, the benefit of the utilization of chance-constraint-based models in the day-ahead operation of a distribution grid is explored in [22,23] to deal with the uncertainty of DERs and risks in the system. In [24], the operational risks introduced by the uncertainty of renewable resources and energy storage systems (ESSs) are controlled by a risk-based chance-constrained method. The stochasticity of DERs is formulated in [25] using a chance-constrained ACOPF to calculate distribution locational marginal prices. Reference [26] uses a chance-constrained model to control the uncertainty of DERs in the hour-ahead model. The robustness level of DERs' investments through a chance-constrained information gap decision model is maximized in [27]. Reference [28] proposes a joint energy and reserve peer-to-peer market to optimize agent revenue while addressing the uncertainty of DERs by a chance-constrained approach. More studies on the optimal operation of distribution grids with uncertainty modeling have been conducted [29–37]. Though these studies (i.e., [22–37]) develop different models to address the uncertainty of DERs, the system operations can be further enhanced by improving the uncertainty modeling based on prosumers' historical data and demographic information.

In light of the above literature review, the main contributions of this paper can be summarized as follows:

- An advanced behavior-aware and socially aware aggregation approach is proposed to properly aggregate the DR resources of prosumers based on their demographic characteristics, the DR program, and time information. The historic consumption patterns and DR of aggregated prosumers based on the proposed socially aware aggregation approach are leveraged in machine learning methods, such as an artificial neural network, to estimate DR and the uncertainty of DR participation. The proposed socially aware aggregation approach is evaluated by comparing the DR uncertainty probability distribution of prosumers with those of a random aggregation.
- A two-stage chance-constrained framework is proposed, which integrates the SOCP-based ACOPF model and different uncertainty distributions of prosumers' behavior, loads, and DERs into one framework. The integration of the socially aware approach and SOCP-based ACOPF into the chance-constrained framework is presented as a risk-aware and socially aware ACOPF model that can mitigate operational risks against potentially expensive real-time prices and ensure the operation of a secure and reliable grid in the distribution system. The model is convex and easy to solve. The computational time of the proposed framework has a nearly linear relationship with the number of scenarios. The PV setpoints and prosumers' behavior for DR programs are optimized to satisfy an acceptable probability violation level for all periods via the chance-constrained framework. A Monte Carlo simulation (MCS) is used to generate scenarios and the OpenDSS power flow tool is used to quickly evaluate the system conditions and chance constraints.

The work of this paper can be summarized in the following flowchart in Figure 1.

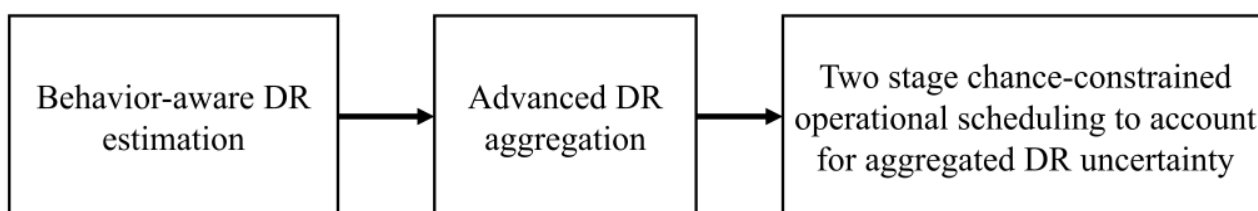


Figure 1. Flowchart of the work and scope of this paper.

The proposed algorithm is tested in a modified IEEE test system. A real historical dataset from a local utility company and the corresponding anonymized demographic information of several thousand residential customers are used for the analysis in the case studies. This paper is outlined as follows. Section 2 explains the socially aware approach and uncertainty modeling of DERs and demand. The proposed two-stage risk-aware and socially aware ACOPF model is delineated in Section 3. The numerical results and computational performance are presented and discussed in Section 4. Finally, Section 5 concludes the paper.

2. Uncertainty Modeling of DERs and Demand

2.1. HITL Factors of DR and Socially Aware Approach

The HITL factors of DR, incorporating the consumption behavior and flexibility of prosumers, are modeled for an uncertainty analysis of the distribution system. A socially aware aggregation method of prosumers is proposed in Algorithm 1 based on response characteristics, selected demographic characteristics, DR programs, and the time of the DR programs to improve the estimation of DR participation and DR uncertainty modeling.

Algorithm 1: Socially Aware Approach.

Create demographic cluster set $O = \{O_1, \dots, O_n\}$.
 for $k = 1, 2, \dots, n$ do

1. Aggregate prosumers belong to O_k , receive off-peak historical data H .
2. Train machine learning models with H and corresponding temperature.
3. Select the trained model M with the highest accuracy.
4. Use M to predict on-peak consumption baseline.
5. Compute DR reductions γ for on-peak periods.
6. Fit γ via Gaussian distribution for different on-peak periods ($t = 1, 2, 3, \dots$) and receive $\mathcal{G}_{O_k,t}$.

end for

This approach hypothesizes that prosumers with similar demographic clusters are more likely to have similar appliances, daily schedules, consumption habits, and flexibilities of consumption. As a result, aggregating prosumers with homogenous demographic characteristics and DR programs for the same period can enhance the estimation of DR participation and DR uncertainty characterization. This hypothesis is evaluated in the case studies by comparing the DR uncertainty of the proposed aggregation strategy with a random aggregation, which is labelled as non-socially aware in this paper.

2.2. Uncertainty of PV Generation and Load

Beta distribution functions are used to model solar irradiance and PV generation in Figure 2, in which a and b are the shape parameters of the beta probability density function (PDF) [38]. The expression of the Beta distribution is shown in Equation (1) for $0 \leq x \leq 1$.

$$f(x | a, b) = \frac{\Gamma(a+b)}{\Gamma(a)\Gamma(b)} x^{a-1} (1-x)^{b-1} \quad (1)$$

where $\Gamma(\cdot)$ is the gamma function, which is a commonly used extension of the factorial function to complex numbers. The gamma function is defined for all complex numbers except non-positive integers, i.e., $\Gamma(n) = (n-1)!$ for every positive integer n .

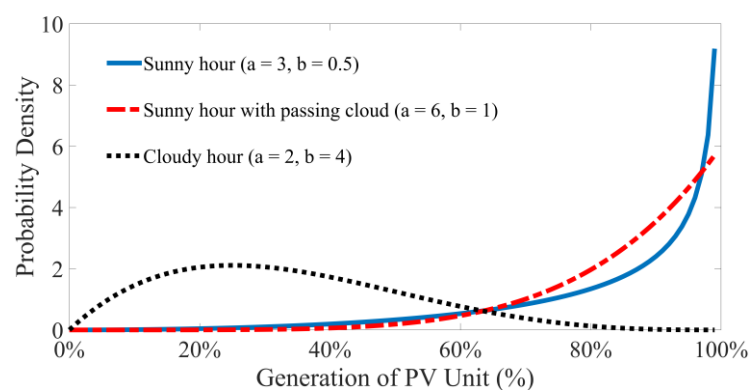


Figure 2. Probability distribution functions of PV generation and weather effect.

As seen in Figure 2, cloudy weather largely affects the PV output. The next day's weather forecasting and the relevant forecasted PV output are used in day-ahead energy and reserve scheduling.

Depending on the weather forecast, suitable beta PDFs are used. For instance, the PDFs shown in Figure 2 are used for a sunny hour, a sunny hour with passing clouds, and a cloudy hour. For the load forecast, the Gaussian distribution function is used to model the forecast error with a zero mean value and 1.5% variance.

3. Proposed Risk-Aware and Socially Aware Chance-Constrained Model

3.1. Convex SOCP-Based ACOPF Model with DERs

Three types of DERs are modeled in this paper, including DR, PV units, and ESSs. The ACOPF is formulated as a convex SOCP problem, which is one of the efficient and exact relaxations for a radial distribution grid [18]. The whole SOCP-based ACOPF model is shown in (2)–(22).

$$\min \sum_{\forall t \in T, \forall g \in G} \left(\rho_t^G P_{g,t}^G + \rho_t^{RG} \mathcal{R}_{g,t}^G \right) + \sum_{\forall t \in T, k \in K} \rho_t^{PV} P_{k,t}^{PV} + \sum_{\forall t \in T, \forall d \in D} \rho_t^{DR} \mathcal{R}_{d,t}^{DR} \quad (2)$$

The objective function in (2) minimizes the total day-ahead operational costs. The first term is the summation of the cost of energy purchased from the upstream wholesale market and the cost of the reserve purchased from the grid. This reserve provides an assurance of energy availability for the DSO/retailer for real-time energy consumption. In this case, the energy and reserve requirements of the DSO/retailer are co-optimized, which results in a more cost-effective solution. The second summation in (2) is the payment to the owners of participating PV units with a positive net power injection to the grid. The last term represents the cost of the reserve provided by DR resources. Without a loss in generalization, reserves are considered in this work to account for the uncertainty of the high penetration of DERs. Note that the reserve provided by DR can be used for real-time energy consumption, by means of direct load control (DLC) or other forms of DR.

$$P_{l,t}^L = g_{i,j} u_{i,t} - g_{i,j} c_{i,j,t} - b_{i,j} e_{i,j,t}, \quad \forall l \in L, \forall t \in T \quad (3)$$

$$Q_{l,t}^L = -b_{i,j} u_{i,t} + b_{i,j} c_{i,j,t} - g_{i,j} e_{i,j,t}, \quad \forall l \in L, \forall t \in T \quad (4)$$

$$c_{i,j,t} = c_{j,i,t}, \quad e_{i,j,t} = -e_{j,i,t}, \quad \forall l \in L, \forall t \in T \quad (5)$$

$$c_{i,j,t}^2 + e_{i,j,t}^2 \leq u_{i,t} u_{j,t}, \quad \forall l \in L, \forall t \in T \quad (6)$$

Active and reactive powers of line l which connect bus i to bus j are expressed by (3)–(4) as linear constraints in terms of three auxiliary variables. If the bus voltage phasor is denoted as $V_{i,t} = |V_{i,t}| \angle \theta_{i,t}$, the nonlinear forms of the three auxiliary variables are given as: $c_{i,j,t} = |V_{i,t}| |V_{j,t}| \cos(\theta_{i,t} - \theta_{j,t})$, $e_{i,j,t} = |V_{i,t}| |V_{j,t}| \sin(\theta_{i,t} - \theta_{j,t})$, and $u_{i,t} = |V_{i,t}|^2$ [16,17]. Due to the nonlinear forms of $c_{i,j,t}$ and $e_{i,j,t}$, constraint (4) is presented to ensure the symmetric and skew-symmetric properties of $c_{i,j,t}$ and $e_{i,j,t}$, respectively. The relationship between three auxiliary variables is $c_{i,j,t}^2 + e_{i,j,t}^2 = u_{i,t} u_{j,t}$, which is non-linear and non-convex. Since introducing non-convexity to the model is not preferred for an ACOPF, this non-convex equation is substituted with an inverted cone (6), which is a convex constraint via SOCP relaxation for radial distribution systems. It should be noted that only when the difference between $u_{i,t} u_{j,t}$ and $c_{i,j,t}^2 + e_{i,j,t}^2$ is sufficiently small, the obtained solution is the exact solution of the system.

$$\left(V_i^L \right)^2 \leq u_{i,t} \leq \left(V_i^U \right)^2, \quad \forall i \in B \setminus G, \forall t \in T \quad (7)$$

$$u_{i,t} = \left(V_i^{sub} \right)^2, \quad \forall i \in G, \forall t \in T \quad (8)$$

$$\left(P_{l,t}^L \right)^2 + \left(Q_{l,t}^L \right)^2 \leq \left(S_l^{L,max} \right)^2, \quad \forall l \in L, \forall t \in T \quad (9)$$

$$0 \leq Q_{q,t}^C \leq Q_q^{C,max}, \quad \forall q, \forall t \quad (10)$$

Voltage limits of buses are imposed by (7) for buses in the distribution grid, while (8) fixes the voltage magnitude for buses connected to the substation. The apparent power

of the branches is constrained by (9). The reactive power injected by the controllable distribution reactive power compensator is constrained by (10).

$$\sum_{\forall k} P_{k,t}^{PV} \leq \alpha_t \sum_{\forall d} P_{d,t}^D, \forall t \in T \quad (11)$$

$$\left(P_{k,t}^{PV}\right)^2 + \left(Q_{k,t}^{PV}\right)^2 \leq \left(S_k^{PV,max}\right)^2, \forall k \in K_a, \forall t \in T \quad (12)$$

$$P_{k,t}^{PV} \leq P_k^{PV,F}, \forall k \in K_b, \forall t \in T \quad (13)$$

$$Q_{k,t}^{PV} = 0, \forall k \in K_b, \forall t \in T \quad (14)$$

The output active power of all PV units is limited by (11) to control the level of uncertainty. The parameter α_t is the participation factor of PV units with respect to the system demand; note that α_t can be greater than one (e.g., in case of a positive net power injection to the transmission system). This constraint ensures that PV power is curtailed, if required, to meet the probability violation requirements as determined by the chance-constrained method. Two types of PV units are modeled in the proposed ACOPT: (i) the inverter of PV type a can provide active and reactive power to meet the load and voltage regulation needs of the system; (ii) PV type b cannot inject reactive power to the grid and operate at a unity power factor providing only active power. The output of PV type a is constrained by (12) as a convex cone while the output of PV type b is limited by (13)–(14).

$$E_{s,t} = E_{s,t-1} - \Delta t P_{s,t}^S, \forall s \in S, \forall t \in T \quad (15)$$

$$E_s^L \leq E_{s,t} \leq E_s^U, \forall s \in S, \forall t \in T \quad (16)$$

$$-P_s^{S,max} \leq P_{s,t}^S \leq P_s^{S,max}, \forall s \in S, \forall t \in T \quad (17)$$

$$E_{s,t=|T|} \geq E_{s,t=1}, \forall s \in S \quad (18)$$

Constraint (15) relates to the state-of-charge (SOC) of ESSs during two consecutive periods. The period duration is Δt , which is considered 1 h in our simulations. Note that $P_{s,t}^S$ is positive if the ESS discharges energy to the system and negative if the ESS is charged. To optimally maintain the ESS's lifetime during its charging and discharging cycles, the SOC limits of the ESS are given by (16), and charging/discharging power is bounded by (17). Constraint (18) ensures that every ESS maintains a SOC at the final period that is not less than that of the first period. Without a loss in generality, this paper assumes that there is no energy loss for the ESS between charging and discharging. However, the ESS efficiency coefficient can also be modeled in the proposed approach.

$$\sum_{\forall g \in Gi} P_{g,t}^G + \sum_{\forall k \in Ki} P_{k,t}^{PV} + \sum_{\forall s \in Si} P_{s,t}^S = \sum_{\forall d \in Di} P_{d,t}^D + \sum_{\forall j \in Bi} P_{i,j,t}^L, \forall i \in B, \forall t \in T \quad (19)$$

$$\sum_{\forall g \in Gi} Q_{g,t}^G + \sum_{\forall k \in Kai} Q_{k,t}^{PV} + \sum_{\forall q \in Ci} Q_{q,t}^C = \sum_{\forall d \in Di} Q_{d,t}^D + \sum_{\forall j \in Bi} Q_{i,j,t}^L, \forall i \in B, \forall t \in T \quad (20)$$

The active power balance at buses is constrained by (19), where Gi , Ki , Si , and Di are sets of substation/grid connections, PVs, ESSs, and demands, respectively, at bus i ; Bi is the set of buses connected to bus i via distribution lines. Similarly, the reactive power balance at buses is ensured by (20), where Kai and Ci are sets of PV type a (with reactive power generation capability) and controllable distribution reactive power compensator, respectively, at bus i .

$$0 \leq \mathcal{R}_{d,t}^{DR} \leq P_{d,t}^{DR,F}, \forall d, \forall t \in T \quad (21)$$

$$\sum_{\forall g \in G} \mathcal{R}_{g,t}^G + \sum_{\forall d \in D} \mathcal{R}_{d,t}^{DR} \geq \zeta^{PV} \sum_{\forall k \in K} P_{k,t}^{PV} + \zeta^D \sum_{\forall d \in D} P_{d,t}^D, \forall t \in T \quad (22)$$

The DR reserve provided by demand d at period t is constrained by (21). In this paper, $P_{d,t}^{DR,F}$ is considered to be forecasted DR (i.e., the average available DR based on different socially aware Gaussian PDFs to which load d belongs). The total reserve requirement is constrained for each period by (22), where the right-hand side is the total required reserve. Coefficients ζ^{PV} and ζ^D are fractions of total PV generation and total demand, respectively. In our simulations, various ζ^{PV} are tested, and ζ^D is fixed to be 5%. Depending on the price of the DR and grid reserves, an optimal portfolio of reserves can be determined by the model. This constraint also self-adjusts the reserves; for instance, when the PV generation is higher, the uncertainty is also higher. Since the total PV generation $\sum_{\forall k} P_{k,t}^{PV}$ becomes higher, a higher reserve is automatically provided and constrained by (22).

3.2. Chance-Constrained Framework of Two-Stage Stochastic Algorithm with Socially Aware Approach

The overall algorithm of the proposed risk-aware and socially aware chance-constrained framework is presented in Figure 3. Stage 1 starts and obtains initial system scheduling and PV participation factor, while Stage 2 ensures a secure and behavior-aware solution of the multi-period energy and reserve scheduling using SOCP-based ACOPF with chance constraints. Stage 1 considers the full capacity of forecasted PV generation and is performed without risk-related chance constraints (23)–(24) in the proposed SOCP-based ACOPF model. Then, the initial PV participation factor α_t is obtained for all the periods without risk evaluations. $R(t) = 1$ is initialized to check all the periods. Note that $R(t) = 1$ refers to a failure in satisfying the probability violation of a chance constraint with a prespecified tolerance. Stage 2 includes an outer loop and an inner loop. The outer loop obtains the multi-period energy and reserve scheduling with different PV participation factors. At the beginning of Stage 2, the outer loop starts with the system scheduling and PV participation factors from Stage 1. Then, Stage 2 goes to the inner loop to check the probability violation of the chance constraints for all periods. In the inner loop, if $R(t) = 1$ for period t , the model utilizes MCS to generate possible scenarios for prosumers' responses to the DR program, PV generation, and the load forecast error using the socially aware uncertainty PDFs, beta PDFs, and Gaussian PDF, respectively. Each scenario is solved by using the OpenDSS power flow tool [30], which can be fast enough to evaluate its operating conditions. Afterward, probability violations are calculated using the maximum likelihood criterion based on OpenDSS results, in terms of the probability of a violation of reserve, voltage, and branch power flows using chance constraints (23), (24), (25), respectively, for the period t .

$$\mathbb{P}\left(\sum_{g \in G} P_{g,t}^G - \sum_{g \in G} P_{g,t}^{sc} \leq \mathcal{R}_t^{sc}\right) \geq 1 - \varepsilon, \forall t \in T \quad (23)$$

$$\mathbb{P}\left(V_i^{min} \leq V_{i,t} \leq V_i^{max}\right) \geq 1 - \varepsilon, \forall i \in B, \forall t \in T \quad (24)$$

$$\mathbb{P}\left(-P_l^{L,max} \leq P_{l,t}^L \leq P_l^{L,max}\right) \geq 1 - \varepsilon, \forall l \in L, \forall t \in T \quad (25)$$

where \mathbb{P} is the probability function; $P_{g,t}^G$ and \mathcal{R}_t^{sc} are the imported active power at connection bus g and the scheduled reserve from the day-ahead SOCP-based ACOPF solution; $P_{g,t}^{sc}$, $V_{i,t}$, and $P_{l,t}^L$ are values obtained from the OpenDSS power flow solutions, indicating the power imported from the grid at connection bus g , the voltage of bus i , and the active power of line l , respectively, at period t . In (23)–(25), ε is the acceptable threshold for the probability of violation (e.g., 3%, 5%, and 8%). The chance constraint (23) limits the probability of facing a large scarcity of reserves. The probability of violating the voltage and line capacity limit due to the uncertainty is restricted by chance constraints (24) and (25), respectively.

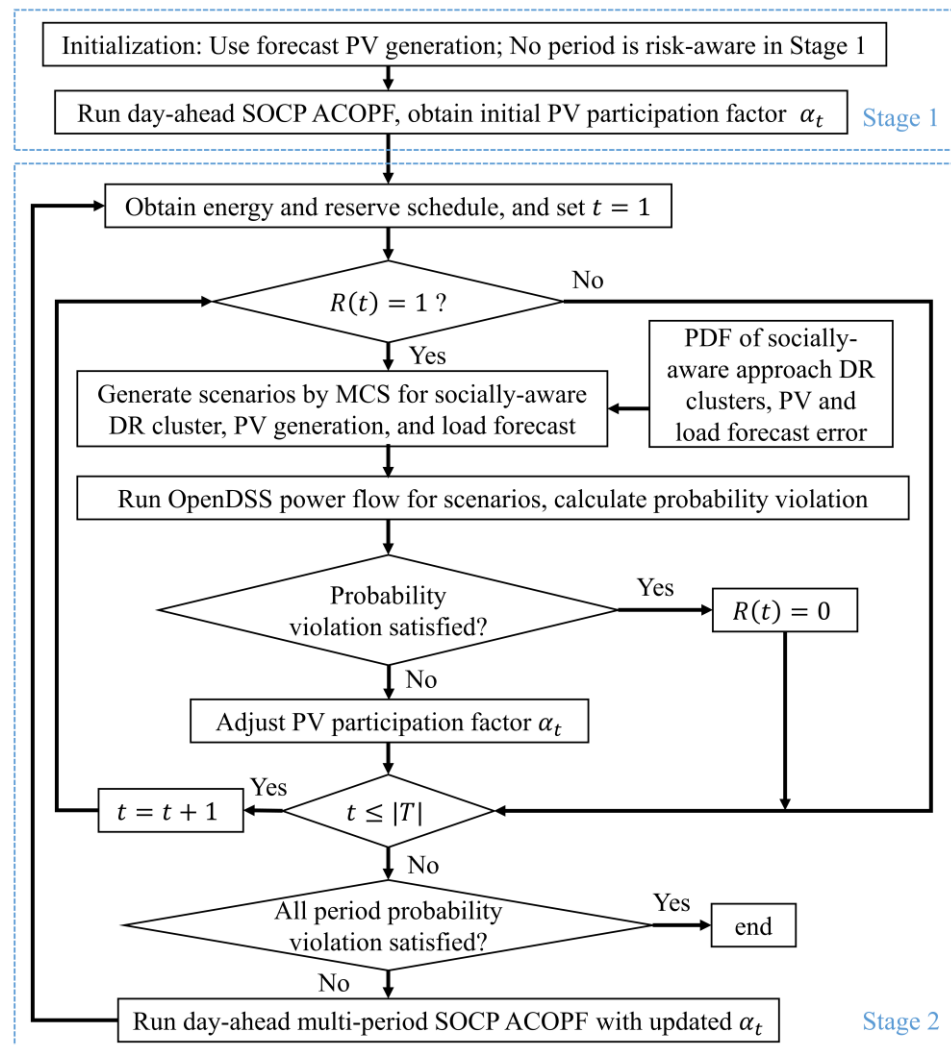


Figure 3. Two-stage flowchart of proposed risk-aware and socially aware algorithm.

If the system probability violations are acceptable within the given tolerance for period t , the risk flag for period t is set as $R(t) = 0$. Otherwise, the PV penetration level is decreased by PV participation factor α_t to reduce the operational risk of this period. After checking the probability violation of the chance constraints for all the periods, the inner loop of Stage 2 is ended. Then, Stage 2 continues its outer loop to run day-ahead multi-period SOCP-based ACOPF with reduced PV participation factors. The outer loop of Stage 2 is ended when all the periods achieve a secure and reliable system operational solution.

The computational burden of the algorithm proposed in Figure 3 mainly depends on the computational time of SOCP-based ACOPF and the number of solved OpenDSS power flows with MCS scenarios. It also depends on the probability violation threshold as if a policy is specified as too risk-averse, it may need more iterations in Stage 2. Obviously, if an appropriate initialization of the PV penetration level is available at the beginning of the algorithm (e.g., from operator experience or a machine learning model trained by historical data), an even smaller number of iterations can be achieved. The proposed algorithm is implemented on an IEEE test system with historical demand and DR data of a local electric utility as discussed in Section 4.

4. Case Studies and Numerical Results

4.1. Uncertainty Modeling with Socially Aware and Non-Socially Aware Aggregation Approaches

The proposed socially aware approach in Section 2 is tested in this subsection. A real dataset of 3750 households, including their historical consumption and temperature, from a local utility company is used for the analysis. The corresponding anonymized demographic information of those prosumers, which is also provided from the local utility, is utilized to aggregate prosumers into a limited number of prosumer clusters, in which the prosumers inside each cluster share similar consumption behaviors. Detailed information on two types of DR programs has been provided in the authors' prior work [12]. By applying the proposed socially aware approach in Algorithm 1, the prosumers' response to the DR program is analyzed and presented in Figure 4 based on their DR data, demographic characteristics, DR program, and time information.

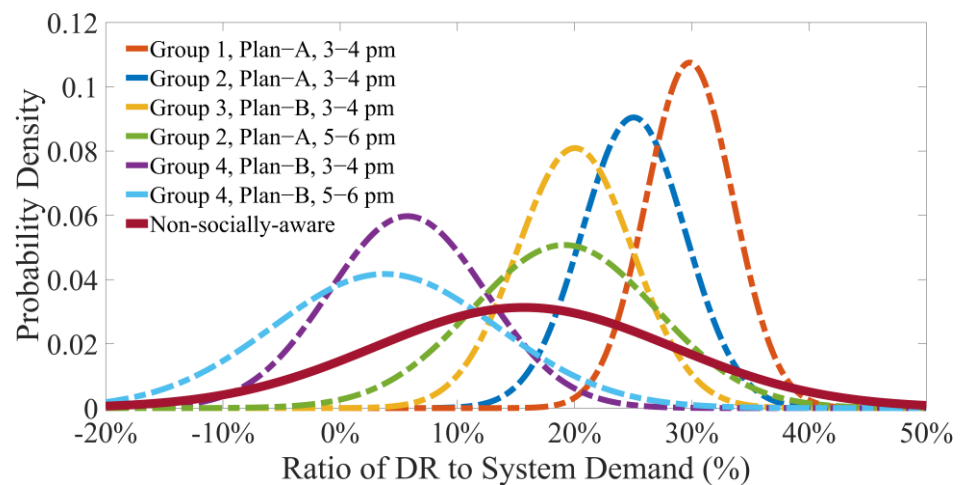


Figure 4. The effect of socially aware aggregation.

In Figure 4, the prosumers' response to DR programs in different sociodemographic clusters and at different times of the day is depicted using the PDF. The legend list in Figure 4 is sorted according to the mean values of the prosumers' responses. Note that a higher variance in the PDFs indicates a higher uncertainty in the prosumers' behavior for DR programs.

As can be seen in Figure 4, all the socially aware clusters (i.e., Group 1–Group 4 with the dashed/dotted line) have a smaller prosumers' response variance and uncertainty compared with those of the non-socially aware (i.e., the curve with a solid line) clusters, which confirms the importance of behavior-aware aggregation. Plan A has a higher on-peak price but a shorter on-peak period than Plan B. The prosumers in Plan A are given higher incentives; thus, they tend to further reduce their consumption during peak hours. For instance, by comparing Group 1 and Group 4 (both with similar demographics and at 3–4 pm), it is found that Plan B prosumers are more reluctant to reduce their consumption. The DR participation of prosumers is correlated with their sociodemographic characteristics. For example, Group 1 has a higher number of people and children than Group 2. By comparing Group 1 and Group 2, it can be observed that households with a higher number of people and children tend to participate more in the DR program under Plan A during the on-peak period from 3 to 4 pm. Moreover, the amount of DR program participation of the prosumers with both plans from 5 to 6 pm is less than that from 3 to 4 pm. For instance, Group 2 at the 5–6 pm interval has higher uncertainty with less DR participation compared to Group 2 at the 3–4 pm time interval. One reason for this might be that people come back home from work at 5–6 pm and need to consume energy (cooking, washing machines, etc.) and are not as concerned about the DR program. Additionally, this period results in a larger variance and higher uncertainties. As seen, Figure 4 reveals the advantage

of the socially aware approach of prosumers in terms of mitigating uncertainty levels as the non-socially aware approach exhibits the highest uncertainty. Thus, a socially aware approach can enable a better assessment and management of uncertainty for the operation of power systems. Moreover, the interpretability of the obtained prosumers' behavior analysis enables the system operator to have more confidence to utilize the DR resources in the distribution grid's operations. The obtained socially aware assessments of prosumers' behavior during the DR programs are embedded into a chance-constrained framework to manage probability violation of the system and ensure a more secure operation in comparison with the non-socially aware approach.

4.2. Test System and Assumptions for Risk-Aware and Socially Aware Chance-Constrained Model

The proposed algorithm is examined on a modified IEEE 33-bus test distribution system to which DR programs, PV, and ESS units are added. The aggregated prosumers' consumption data from a local electric utility company on 16 August 2018 are scaled based on the existing load in the IEEE 33-bus system to model the DR provided by loads. Without a loss in generality, it is assumed that all the prosumers connected to a bus belong to a similar cluster in terms of their consumption behavior. This assumption can be modified by using a percentage of prosumers belonging to each sociodemographic cluster. The PDFs used for the load reduction due to DR programs have been shown in Figure 4 for both socially aware and non-socially aware approaches. Since weather conditions affect PV generation, the weather data of the San Francisco area on 16 August 2018 are used. According to this weather data, the simulation day is sunny throughout the day except for some passing clouds at 5 am, 11 am, and 7 pm. Depending on the forecasted weather conditions, different beta PDFs are used, as explained in Figure 2, in which the curve ($a = 6$, $b = 1$) represents the uncertainty of the PV generation at 5 am, 11 am, and 7 pm, while the curve ($a = 3$, $b = 0.5$) is used for the rest of the day.

The convex SOCP-based ACOPF model is programmed in Python and solved by using CPLEX. All simulations are conducted via a laptop with a 5 GHz CPU and 16GB DDR4. The computational performance is discussed in Section 4.4. The power flow in Figure 3 is solved by OpenDSS, which is a software tool developed by the Electric Power Research Institute (EPRI) for distribution system analyses [39]. For the PV generation price, the net surplus compensation rate in August 2018 is used from the Pacific Gas and Electric (PG&E), which is a utility in California [40]. For the wholesale electricity prices of the upstream grid, the LMP of the California Independent System Operator (CAISO) for the PG&E area on 16 August 2018 is used [41]. For the PV penetration levels, the impact of different seasons is simulated for Phoenix, Arizona. During the spring months, the PV generation is higher than the demand in some periods. During the hot summer months in the Phoenix area, the demand surpasses the PV generation due to the high energy consumption of air conditioners.

Two cases are assumed in our simulations: Case I represents the high penetration level of PV generations in the summer months, while Case II represents an extremely high PV penetration in the spring season in the Phoenix area. The forecasted day-ahead PV generation profiles are depicted in Figure 5 for Cases I and II. The forecasted PV generation of Case I is less than the system's total demand throughout all the periods of the day. The PV generation of Case II is higher than the total load from 9:00 to 14:00. Figure 5 also shows the total day-ahead load profile as well as the wholesale electricity price of the upstream grid and PV power price. The forecasted PV profiles represent the maximum available PV generation. This generation may be curtailed by the proposed chance-constrained framework to maintain an acceptable probability violation of system operation as explained in Section 3.2.

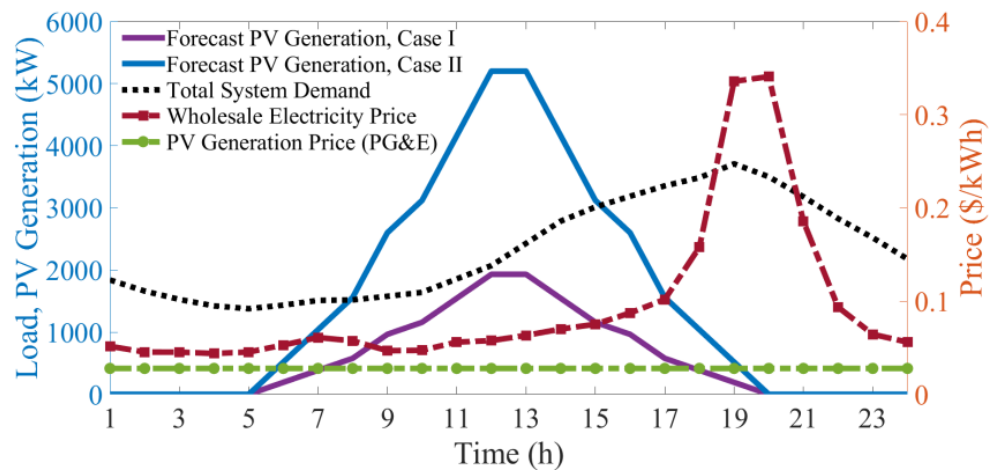


Figure 5. Forecast PV generation for Case I and II, total demand, wholesale power price, and PV power price.

4.3. Simulation Results

In Case I and Case II explained above, the performance of the proposed two-stage algorithm is evaluated via different PV penetration levels. The benefit of utilizing the socially aware approach in the chance-constrained framework is observed in Figures 6 and 7, assuming a 10% reserve policy for both cases. As seen in Figure 6, the scheduled PV power is higher when the socially aware approach (three solid curves) of prosumers is considered compared to the non-socially aware approach (dashed curves) at the same probability violation level (e.g., 3%, 5%, and 8%). This is because the socially aware method allows the assessment, scheduling, and utilization of DR resources’ potential from prosumers with less uncertainty. The reserve scheduled from the DR resources using a socially aware approach is more effective for mitigating operational risks of the system. Due to a smaller variance of PDFs indicating a lower uncertainty of DR (Figure 4), when the socially aware approach is used, even with the most conservative probability violation level (3%), the socially aware approach can integrate higher PV energy than the non-socially aware approach under the most optimistic probability violation threshold (8%) as shown in Figures 6 and 7.

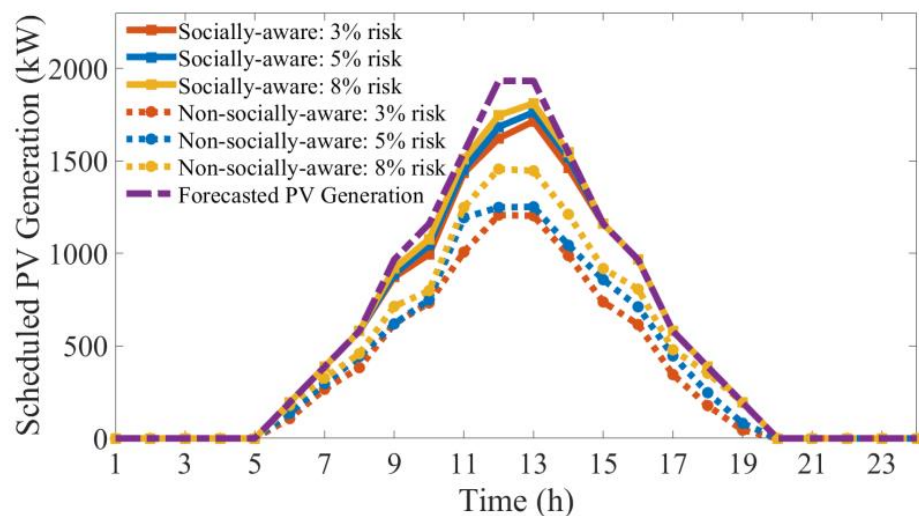


Figure 6. Scheduled PV generation for Case I with PV reserve policy of 10%.

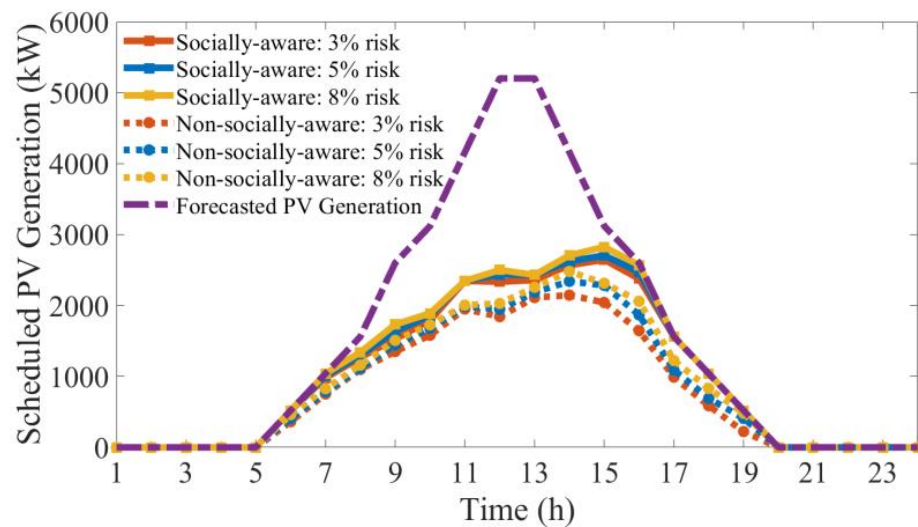


Figure 7. Scheduled PV generation for Case II with PV reserve policy of 10%.

In addition, the price of using PV units is lower than that of the grid power at all periods as seen in Figures 6 and 7. The model prefers to utilize PV generation as much as possible as the objective function minimizes the total system cost. However, the higher the PV generation, the higher the uncertainty and operating risk level. Therefore, the proposed two-stage algorithm with different approaches (socially aware or non-socially aware) curtails some of the PV generation of a certain level to maintain the operating risk level lower than the given probability violation threshold of the chance constraints. This curtailment is substantially less when using a socially aware scheduling approach. The consideration of prosumers' sociodemographic information as part of the HITL feature and chance-constrained framework enhances the integration of green energy resources, lowers the total operational cost, and improves distribution grid operations.

To investigate the effect of PV reserve policy and the probability violation threshold of chance constraints on the scheduled PV energy, a sensitivity analysis is conducted and presented in Tables 1 and 2, in which the scheduled PV energy in the test system of the day-ahead scheduling is presented for the non-socially aware and socially aware approaches. For convenience, the percentages of energy values are also given (with respect to the lowest energy value 7534 kWh in Table 1 and 15,573 kWh in Table 2). As the probability violation threshold increases from 3% to 8%, the scheduled PV energy increases for both Case I and Case II because a large probability violation threshold refers to an optimistic operation, which can lead to scheduling a greater amount of PV energy in the system. Furthermore, increasing the PV reserve policy from 5% to 15% results in higher scheduled PV energy in both cases. This is expected because higher amounts of the reserve are considered to account for the uncertainty, which then increases the scheduled PV energy. As seen in these tables, the proposed socially aware approach outperforms the conventional non-socially aware method in terms of scheduled PV energy in all combinations of PV reserve policy and probability violation threshold for Case I and Case II. The largest benefit of the proposed socially aware approach can be seen in Case II (the row with the bold font in Table 2), in which the difference in the PV energy scheduled with the socially aware and non-socially aware approaches is $166\% - 131\% = 35\%$ ($25797 - 20380 = 5417$ kW). In addition, PV energy curtailments are shown in Tables 1 and 2. As can be seen, socially aware approaches can always achieve a lower PV curtailment compared to a non-socially aware approach. Moreover, PV energy curtailment by using socially aware approaches can even reach zero as shown in Table 1.

Table 1. Total Scheduled PV Energy for Case I.

PV Reserve Policy (%)	Probability Violation Threshold	Non-Socially Aware PV Energy (kWh)	Socially Aware PV Energy (kWh)	Non-Socially Aware PV Energy Curtailment (kWh)	Socially Aware PV Energy Curtailment (kWh)
5%	3%	7534 (100%)	10,802 (143%)	5989	2721
5%	5%	8169 (108%)	11,227 (149%)	5354	2296
5%	8%	8611 (114%)	11,840 (157%)	4912	1683
10%	3%	8429 (112%)	12,539 (166%)	5094	984
10%	5%	9320 (124%)	12,789 (170%)	4203	734
10%	8%	10,583 (140%)	13,048 (173%)	2940	475
15%	3%	10,922 (145%)	13,444 (178%)	2601	79
15%	5%	12,018 (160%)	13,523 (179%)	1505	0
15%	8%	12,574 (167%)	13,523 (179%)	949	0

Table 2. Total Scheduled PV Energy for Case II.

PV Reserve Policy (%)	Probability Violation Threshold	Non-Socially Aware PV Energy (kWh)	Socially Aware PV Energy (kWh)	Non-Socially Aware PV Energy Curtailment (kWh)	Socially Aware PV Energy Curtailment (kWh)
5%	3%	15,573 (100%)	20,604 (132%)	20,834	15,803
5%	5%	16,426 (105%)	21,161 (136%)	19,981	15,246
5%	8%	17,307 (111%)	21,811 (140%)	19,100	14,596
10%	3%	18,684 (120%)	23,835 (153%)	17,723	12,572
10%	5%	20,230 (130%)	24,460 (157%)	16,177	11,947
10%	8%	21,373 (137%)	25,026 (161%)	15,034	11,381
15%	3%	20,380 (131%)	25,797 (166%)	16,027	10,610
15%	5%	21,305 (137%)	25,860 (166%)	15,102	10,547
15%	8%	21,801 (140%)	25,938 (167%)	14,606	10,469

In Tables 3 and 4, total operation costs under different PV reserve policies and probability violation thresholds are given for Case I and Case II regarding the socially aware and non-socially aware methods. In order to report the percentage values to make comparisons, the cost values are normalized by USD 5499 and USD 4863, which are the lowest values in Tables 3 and 4, respectively. As seen in Tables 3 and 4, the operation cost is always lower under the socially aware method. The largest amount saved is $110.71\% - 102.88\% = 7.83\%$, which is related to the bold row in Table 4. The reduction in the operation cost is because the proposed socially aware method can employ the DR potential of prosumers more effectively and utilize less expensive PV energy.

Table 3. Total System Operation Cost for Case I.

PV Reserve Policy (%)	Probability Violation Threshold	Non-Socially Aware Cost (USD)	Socially Aware Cost (USD)
5%	3%	5776 (105.04%)	5569 (101.27%)
5%	5%	5717 (103.96%)	5557 (101.05%)
5%	8%	5685 (103.38%)	5538 (100.71%)
10%	3%	5740 (104.38%)	5522 (100.42%)
10%	5%	5685 (103.38%)	5515 (100.29%)
10%	8%	5598 (101.80%)	5507 (100.15%)
15%	3%	5656 (102.86%)	5501 (100.04%)
15%	5%	5579 (101.45%)	5499 (100.00%)
15%	8%	5537 (100.69%)	5499 (100.00%)

Table 4. Total System Operation Cost for Case II.

PV Reserve Policy (%)	Probability Violation Threshold	Non-Socially Aware Cost (USD)	Socially Aware Cost (USD)
5%	3%	5384 (110.71%)	5003 (102.88%)
5%	5%	5315 (109.29%)	4983 (102.47%)
5%	8%	5246 (107.88%)	4958 (101.95%)
10%	3%	5239 (107.73%)	4902 (100.80%)
10%	5%	5113 (105.14%)	4882 (100.39%)
10%	8%	5031 (103.45%)	4863 (100.00%)
15%	3%	5155 (106.00%)	4863 (100.00%)
15%	5%	5077 (104.40%)	4863 (100.00%)
15%	8%	5069 (104.24%)	4864 (100.00%)

4.4. Computational Performance

In this subsection, the computational performance of the proposed risk-aware socially aware chance-constrained model is discussed. Solving a one-hour and a 24-hour SOCP-based ACOFP model (2)–(22) takes 0.46 and 1.77 s, respectively. The computational time to solve the two-stage socially aware chance-constrained SOCP-based ACOFP model with a different number of MCS scenarios is shown in Tables 5 and 6 for the one-hour and the 24-hour system operation scheduling based on Case I with a 10% PV reserve policy and a 5% probability violation threshold.

Table 5. Computational Performance of the Proposed Model for One Time Interval.

Cases	Time (s)
1000 MCS scenarios	9.01
100 MCS scenarios	0.99

Table 6. Computational Performance of the Proposed Model for Day-ahead Scheduling.

Cases	Time (s)
1000 MCS scenarios	579.3
500 MCS scenarios	276.6
200 MCS scenarios	109.4
100 MCS scenarios	76.3

The computational time for solving the whole process of the two-stage algorithm is very short in Table 5 because using OpenDSS as a tool to solve the power flow to check the probability violation of chance constraints is sufficiently fast. Therefore, under the proposed chance-constrained framework, the security and reliability of the system operating condition can be quickly evaluated. As shown in Table 6, solving the whole two-stage algorithm for a 24-hour system operational scheduling with the uncertainty of DERs is still computationally efficient. The computational time has a linear relationship with the number of scenarios in the MCS process. If 1000 scenarios are considered in the MCS process to check the probability violation of the system, the proposed algorithm only needs to take less than 10 min to solve it and obtains an optimal solution that ensures a secure and reliable operation of the system. In comparison with some other robust optimization models that need more than 2 h to solve, such as those in [18,19], the proposed chance-constrained framework is computationally efficient and easy to solve. Moreover, if an appropriate initialization of the PV participation factor is available at Stage 1 of the algorithm presented in Figure 3 (e.g., from operator experience or a machine learning model trained by historical data), an even lower computational time can be achieved. Furthermore, the evaluation of the scenarios in OpenDSS can be performed using parallel computing, which further enhances the tractability of the proposed approach.

5. Conclusions

In this paper, behavior-aware and socially aware approaches are proposed for the enhanced modeling of prosumers' behavior in DR programs and their uncertainty. To employ the DR potential of prosumers, the socially aware approach classifies prosumers into clusters considering their prior responses, selected demographic characteristics, DR programs, and the time of day (HITL features). The proposed socially aware approach is a general analytic structure that can model different prosumers' behaviors in the utility area. Moreover, the assessment of prosumers' behaviors during DR programs enables system operators to have more confidence in the utilization of DR resources in the operation of distribution grids. The convex SOCP-based ACOFP is used for the distribution system. A chance-constrained framework is proposed to account for the uncertainty in the distribution network. To manage uncertainties introduced by DERs and load forecast errors, a chance-constrained framework is constructed as a two-stage algorithm for the day-ahead energy and reserve scheduling of distribution grids. The chance-constrained framework is intuitive and easy to solve. The integration of a socially aware approach, convex SOCP-based ACOFP, and chance-constrained framework is presented as an iterative risk-aware and socially aware algorithm in the case study to ensure a secure and reliable system operation in the distribution grids with a high penetration of DERs.

The socially aware approach increases the utilization of available PV generation in the distribution system with the same PV reserve policy and risk threshold. This is because the socially aware approach enables the scheduling and utilization of DR with less uncertainty stemming from prosumers' behavior. Moreover, the proposed socially aware approach outperforms the conventional non-socially aware method in terms of scheduled PV energy in all combinations of the PV reserve policy and probability violation threshold for the two different case studies. The socially aware approach reduces system operation costs due to its effective utilization of DERs, which results in an enhancement of social welfare. The proposed algorithm is intuitive and easy to solve. The computational time of the two-stage algorithm has a nearly linear relationship with the number of evaluated scenarios.

Since distribution grids are commonly three-phase unbalanced networks, the three-phase unbalanced convex ACOFP with the proposed chance-constrained framework will be studied in our future work. More demographic clusters should be tested via the proposed socially aware approach. In addition, PV units installed with a Volt-VAR controller should also be investigated due to the issued IEEE Standard 1547-2018, which requires an improvement in the representation of DERs in distribution operations.

Author Contributions: Conceptualization, M.H. and M.K.; Methodology, M.H., Z.S. and M.K.; Data, A.D. and P.M.; Analysis, M.H.; Validation, M.H., Z.S. and M.K.; Writing—Original Draft, M.H.; Writing—Review and editing, M.H., Z.S., M.K. and M.E. All authors have read and agreed to the published version of the manuscript.

Funding: This research received no external funding.

Data Availability Statement: Data sharing not applicable.

Conflicts of Interest: The authors declare no conflict of interest.

Nomenclature

Indices and Sets

$d \in D$	Index and set of demands.
$g \in G$	Index and set of buses connected to the substation.
$i \in B$	Index and set of buses.
$l \in L$	Index and set of lines.
$k \in K$	Index and set of all photovoltaic (PV) units.
$q \in C$	Index and set of controllable distribution reactive power compensator.
$s \in S$	Index and set of energy storage systems.

$t \in T$	Index and set of time.
K_a, K_b	Sets of PV types a and b , respectively.
Parameters	
ρ_t^G, ρ_t^{PV}	Energy cost from bulk system and PV, respectively, at time t (\$/kWh).
ρ_t^{RG}, ρ_t^{DR}	Reserve cost from bulk system and demand response, respectively, at time t (\$/kWh).
α_t	Participation factor of all PV units at time t .
μ_d, σ_d	Mean and standard deviation of demand response for demand d .
ζ^{PV}, ζ^D	Fractions of required reserve for uncertainty of PV generation and load, respectively.
b_l	Susceptance of branch l .
g_l	Conductance of branch l .
E_s^L, E_s^U	Lower and upper energy capacity limits of energy storage system s .
$P_{d,t}^D, Q_{d,t}^D$	Active and reactive power demand d at time t .
$P_{d,t}^{DR,F}$	Forecasted demand response d at time t .
$P_{k,t}^{PV,F}$	Forecasted output power of PV unit k at time t .
$P_s^{S,max}$	Maximum charging/discharging limit of energy storage system s .
$Q_q^{C,max}$	Rating of controllable distribution reactive power compensator q .
$S_l^{L,max}$	Apparent power rating of branch l .
$S_k^{PV,max}$	Inverter rating of PV unit k .
V_i^L, V_i^U	Lower and upper voltage magnitude limits at bus i .
Decision Variables	
$c_{i,j,t}, e_{i,j,t}$	Auxiliary variables used for convexification.
$u_{i,t}$	Auxiliary variable used for convexification.
$E_{s,t}$	Stored energy of energy storage system s at time t .
$P_{g,t}^G, Q_{g,t}^G$	Active and reactive power from bulk system in bus g at time t .
$P_{l,t}^L$	Active power of branch l at time t .
$P_{k,t}^{PV}, Q_{k,t}^{PV}$	Active and reactive power of PV k at time t .
$P_{s,t}^S$	Active power output of energy storage system s at time t .
Q_q^C	Reactive power of controllable distribution reactive power compensator q at time t .
$Q_{l,t}$	Reactive power of branch l at time t .
$\mathcal{R}_{d,t}^{DR}$	Demand response reserve from demand d at time t .
$\mathcal{R}_{g,t}^G$	Reserve from bulk system in bus g at time t .

References

1. Percy, S.D.; Aldeen, M.; Berry, A. Residential Demand Forecasting with Solar-Battery Systems: A Survey-Less Approach. *IEEE Trans. Sustain. Energy* **2018**, *9*, 1499–1507. [\[CrossRef\]](#)
2. Zhang, Y.; Chen, W.; Xu, R.; Black, J. A Cluster-Based Method for Calculating Baselines for Residential Loads. *IEEE Trans. Smart Grid*. **2016**, *7*, 2368–2377. [\[CrossRef\]](#)
3. Capasso, A.; Grattieri, W.; Lamedica, R.; Prudenzi, A. A Bottom-up Approach to Residential Load Modeling. *IEEE Trans. Power Syst.* **1994**, *9*, 957–964. [\[CrossRef\]](#)
4. Alonso, A.M.; Nogales, F.J.; Ruiz, C. Hierarchical Clustering for Smart Meter Electricity Loads Based on Quantile Autocovariances. *IEEE Trans. Smart Grid*. **2020**, *11*, 4522–4530. [\[CrossRef\]](#)
5. Eksin, C.; Deliç, H.; Ribeiro, A. Demand Response Management in Smart Grids with Heterogeneous Consumer Preferences. *IEEE Trans. Power Syst.* **2015**, *6*, 3082–3094. [\[CrossRef\]](#)
6. Gao, J.; Ma, Z.; Yang, Y.; Gao, F.; Guo, G.; Lang, Y. The Impact of Customers' Demand Response Behaviors on Power System with Renewable Energy Sources. *IEEE Trans. Sustain. Energy* **2020**, *11*, 2581–2592. [\[CrossRef\]](#)
7. Meng, F.; Zeng, X. A Profit Maximization Approach to Demand Response Management with Customers Behavior Learning in Smart Grid. *IEEE Trans. Smart Grid*. **2016**, *7*, 1516–1529. [\[CrossRef\]](#)
8. Gan, L.; Li, N.; Topcu, U.; Low, S.H. Exact Convex Relaxation of Optimal Power Flow in Radial Networks. *IEEE Trans. Autom. Control*. **2015**, *60*, 72–87. [\[CrossRef\]](#)
9. Huang, S.; Wu, Q.; Wang, J.; Zhao, H. A Sufficient Condition on Convex Relaxation of AC Optimal Power Flow in Distribution Networks. *IEEE Trans. Power Syst.* **2017**, *32*, 1359–1368. [\[CrossRef\]](#)
10. Lavaei, J.; Low, S.H. Zero Duality Gap in Optimal Power Flow Problem. *IEEE Trans. Power Syst.* **2012**, *27*, 92–107. [\[CrossRef\]](#)
11. Low, S.H. Convex Relaxation of Optimal Power Flow—Part I: Formulations and Equivalence. *IEEE Trans. Control Netw. Syst.* **2014**, *1*, 15–27. [\[CrossRef\]](#)
12. He, M.; Khorsand, M. A Data-Driven Based Strategy to Evaluate Participation of Diverse Social Classes in Smart Electric Grids. In Proceedings of the 2019 North American Power Symposium (NAPS), Wichita, KS, USA, 13–15 October 2019; pp. 1–6.

13. Steen, D.; Tuan, L.A.; Carlson, O.; Bertling, L. Assessment of Electric Vehicle Charging Scenarios Based on Demographical Data. *IEEE Trans. Smart Grid.* **2012**, *3*, 1457–1468. [[CrossRef](#)]
14. Albert, A.; Rajagopal, R. Smart Meter Driven Segmentation: What Your Consumption Says About You. *IEEE Trans. Power Syst.* **2013**, *28*, 4019–4030. [[CrossRef](#)]
15. Federal Energy Regulatory Commission (FERC), USA. FERC Order 2222. Available online: https://www.energy.gov/sites/default/files/2021-04/EAC%20FERC%20Order%202222%20Recommendations%202021-04-15_finalDraft.pdf (accessed on 7 December 2022).
16. Jabr, R.A. Radial Distribution Load Flow Using Conic Programming. *IEEE Trans. Power Syst.* **2006**, *21*, 1458–1459. [[CrossRef](#)]
17. Farivar, M.; Low, S.H. Branch Flow Model: Relaxations and Convexification—Part II. *IEEE Trans. Power Syst.* **2013**, *28*, 2565–2572. [[CrossRef](#)]
18. Liu, Y.; Li, J.; Wu, L.; Ortmeyer, T. Chordal Relaxation Based ACOPF for Unbalanced Distribution Systems with DERs and Voltage Regulation Devices. *IEEE Trans. Power Syst.* **2018**, *33*, 970–984. [[CrossRef](#)]
19. Fu, L.; Liu, B.; Meng, K.; Dong, Z.Y. Optimal Restoration of An Unbalanced Distribution System into Multiple Microgrids Considering Three-Phase Demand-Side Management. *IEEE Trans. Power Syst.* **2021**, *36*, 1350–1361. [[CrossRef](#)]
20. Lorca, A.; Sun, X.A. The Adaptive Robust Multi-Period Alternating Current Optimal Power Flow Problem. *IEEE Trans. Power Syst.* **2018**, *33*, 1993–2003. [[CrossRef](#)]
21. Soares, T.; Bessa, R.J.; Pinson, P.; Morais, H. Active Distribution Grid Management Based on Robust AC Optimal Power Flow. *IEEE Trans. Smart Grid.* **2018**, *9*, 6229–6241. [[CrossRef](#)]
22. Geng, X.; Xie, L. Data-Driven Decision Making with Probabilistic Guarantees (Part 1): A Schematic Overview of Chance-Constrained Optimization. Available online: <https://arxiv.org/pdf/1903.10621.pdf> (accessed on 7 December 2022).
23. Geng, X.; Xie, L. Data-Driven Decision Making with Probabilistic Guarantees (Part 2): Applications of Chance-Constrained Optimization in Power Systems. Available online: <https://arxiv.org/pdf/1904.06755.pdf> (accessed on 7 December 2022).
24. Amini, M.; Almassalkhi, M. Optimal Corrective Dispatch of Uncertain Virtual Energy Storage Systems. *IEEE Trans. Smart Grid.* **2020**, *11*, 4155–4166. [[CrossRef](#)]
25. Mieth, R.; Dvorkin, Y. Distribution Electricity Pricing under Uncertainty. *IEEE Trans. Power Syst.* **2020**, *35*, 2325–2338. [[CrossRef](#)]
26. Zhang, H.; Hu, Z.; Munsing, E.; Moura, S.J.; Song, Y. Data-Driven Chance-Constrained Regulation Capacity Offering for Distributed Energy Resources. *IEEE Trans. Smart Grid.* **2019**, *10*, 2713–2725. [[CrossRef](#)]
27. Cao, X.; Wang, J.; Zeng, B. A Chance Constrained Information-Gap Decision Model for Multi-Period Microgrid Planning. *IEEE Trans. Power Syst.* **2018**, *33*, 2684–2695. [[CrossRef](#)]
28. Guo, Z.; Pinson, P.; Chen, S.; Yang, Q.; Yang, Z. Chance-Constrained Peer-to-Peer Joint Energy and Reserve Market Considering Renewable Generation Uncertainty. *IEEE Trans. Smart Grid.* **2021**, *12*, 798–809. [[CrossRef](#)]
29. Sadati, S.M.B.; Moshtagh, J.; Shafie-khah, M.; Rastgou, A.; Catalão, J.P. Operational scheduling of a smart distribution system considering electric vehicles parking lot: A bi-level approach. *Int. J. Electr. Power Energy Syst.* **2019**, *105*, 159–178. [[CrossRef](#)]
30. Esmaili, S.; Anvari-Moghaddam, A.; Jadid, S.; Guerrero, J.M. A stochastic model predictive control approach for joint operational scheduling and hourly reconfiguration of distribution systems. *Energies* **2018**, *11*, 1884. [[CrossRef](#)]
31. Sadati, S.M.B.; Moshtagh, J.; Shafie-khah, M.; Catalão, J.P. Smart distribution system operational scheduling considering electric vehicle parking lot and demand response programs. *Electr. Power Syst. Res.* **2018**, *160*, 404–418. [[CrossRef](#)]
32. Esmaili, S.; Anvari-Moghaddam, A.; Jadid, S. Optimal operational scheduling of reconfigurable multi-microgrids considering energy storage systems. *Energies* **2019**, *12*, 1766. [[CrossRef](#)]
33. Zakariazadeh, A.; Jadid, S.; Siano, P. Multi-objective scheduling of electric vehicles in smart distribution system. *Energy Convers. Manag.* **2014**, *79*, 43–53. [[CrossRef](#)]
34. Sperstad, I.B.; Korpås, M. Energy storage scheduling in distribution systems considering wind and photovoltaic generation uncertainties. *Energies* **2019**, *12*, 1231. [[CrossRef](#)]
35. Zakariazadeh, A.; Jadid, S.; Siano, P. Economic-environmental energy and reserve scheduling of smart distribution systems: A multiobjective mathematical programming approach. *Energy Convers. Manag.* **2014**, *78*, 151–164. [[CrossRef](#)]
36. Umeozor, E.C.; Trifkovic, M. Operational scheduling of microgrids via parametric programming. *Appl. Energy* **2016**, *180*, 672–681. [[CrossRef](#)]
37. Zamani, A.G.; Zakariazadeh, A.; Jadid, S.; Kazemi, A. Stochastic operational scheduling of distributed energy resources in a large scale virtual power plant. *Int. J. Electr. Power Energy Syst.* **2016**, *82*, 608–620. [[CrossRef](#)]
38. Fatemi, S.A.; Kuh, A.; Fripp, M. Parametric Methods for Probabilistic Forecasting of Solar Irradiance. *Renew. Energy* **2018**, *129*, 666–676. [[CrossRef](#)]
39. Electric Power Research Institute (EPRI). Simulation Tool—OpenDSS. Available online: <https://smartgrid.epri.com/SimulationTool.aspx> (accessed on 7 December 2022).
40. Pacific Gas and Electric (PG&E), CA, USA. Net Surplus Compensation Rates for Energy. Available online: https://www.pge.com/pge_global/common/pdfs/solar-and-vehicles/green-energy-incentives/AB920_RateTable.pdf (accessed on 7 December 2022).
41. California ISO (CAISO), CA, USA. Market Price Map. Available online: <http://www.caiso.com/PriceMap/Pages/default.aspx> (accessed on 7 December 2022).